

Supporting Information

Preparation of a Sulfur-Functionalized Microporous Polymer Sponge and *in situ* Growth of Silver Nanoparticles: a Compressible Monolithic Catalyst

Jong Gil Kim, Min Chul Cha, Jeongmin Lee, Taejin Choi, and Ji Young Chang*

Department of Materials Science and Engineering, College of Engineering, Seoul National
University, Seoul 08826, Korea

E-mail: jichang@snu.ac.kr

Table S1. Elemental compositions of the MOP sponge and S-MOPS measured by elemental analysis.

	C (wt%)	H (wt%)	S (wt%)
the MOP sponge	67.6	1.8	0
S-MOPS	66.4	2.6	14.1

Table S2. Examples of monolithic catalysts for the reduction of 4-nitrophenol.

	M_{act}	Support	$k (s^{-1}) * 10^{-3}$	Reference
S-MOPS-Ag	Ag	MOP	7.61	This work (with the compression-release process)
Au-DA-polyHIPE	Au	polyHIPE	6.3	1
Ag/carbon	Ag	carbon	4.92	2
Pt-polyHIPE	Pt	polyHIPE	3.5	3

M_{act} : active metal, polyHIPE: poly(high internal phase emulsion)

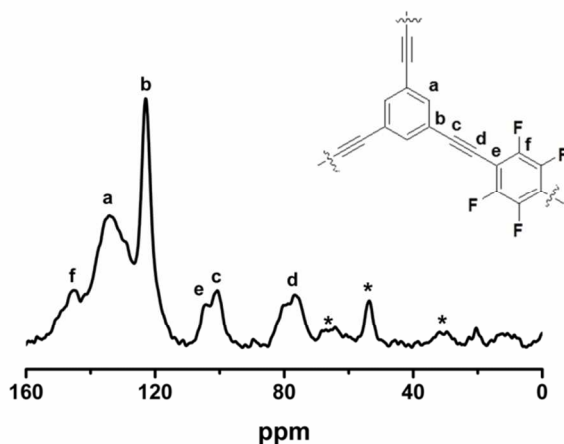


Figure S1. Solid state ^{13}C CP/MAS NMR spectrum of the MOP sponge.

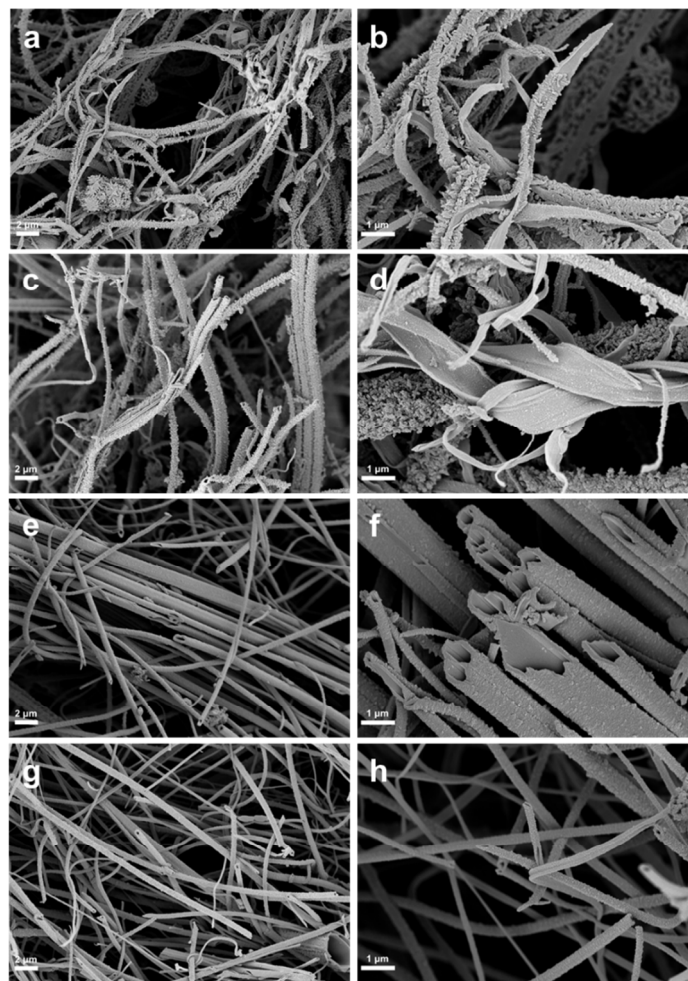


Figure S2. SEM images of the MOP sponge measured after a reaction time of (a, b) 1h, (c, d) 1.5 h, (e, f) 2 h, and (g, h) 3 h.

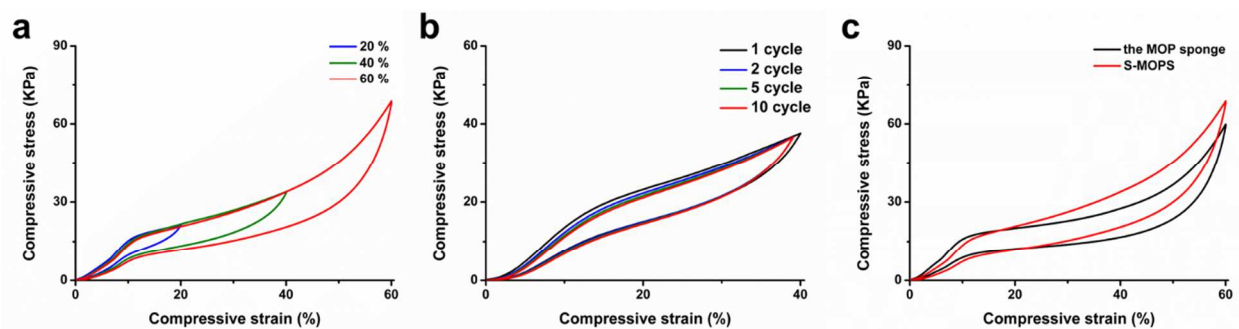


Figure S3. a) Compressive stress-strain curves (maximum strain = 20, 40 and 60 %) and b) 10 cycles of the loading-unloading test results of S-MOPS (maximum strain = 40 %). c) Comparison of hysteresis curves of the MOP sponge and S-MOPS at 40 %.

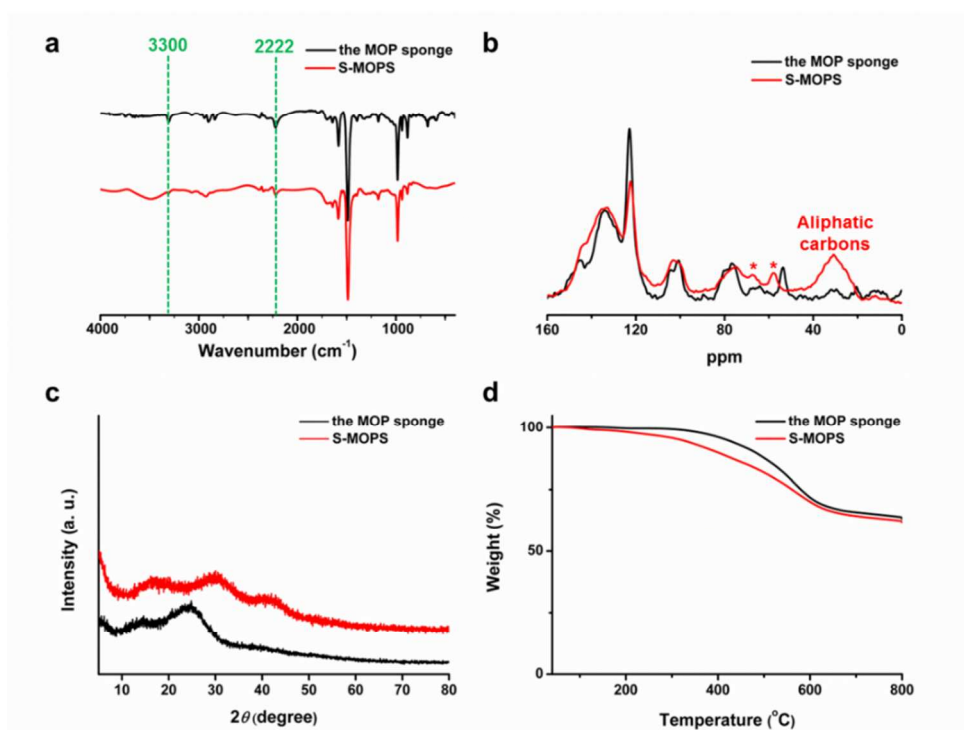


Figure S4. a) FT-IR spectra, b) Solid state ^{13}C CP/MAS NMR spectra, c) PXRD patterns and d) TGA thermograms of the MOP sponge and S-MOPS.

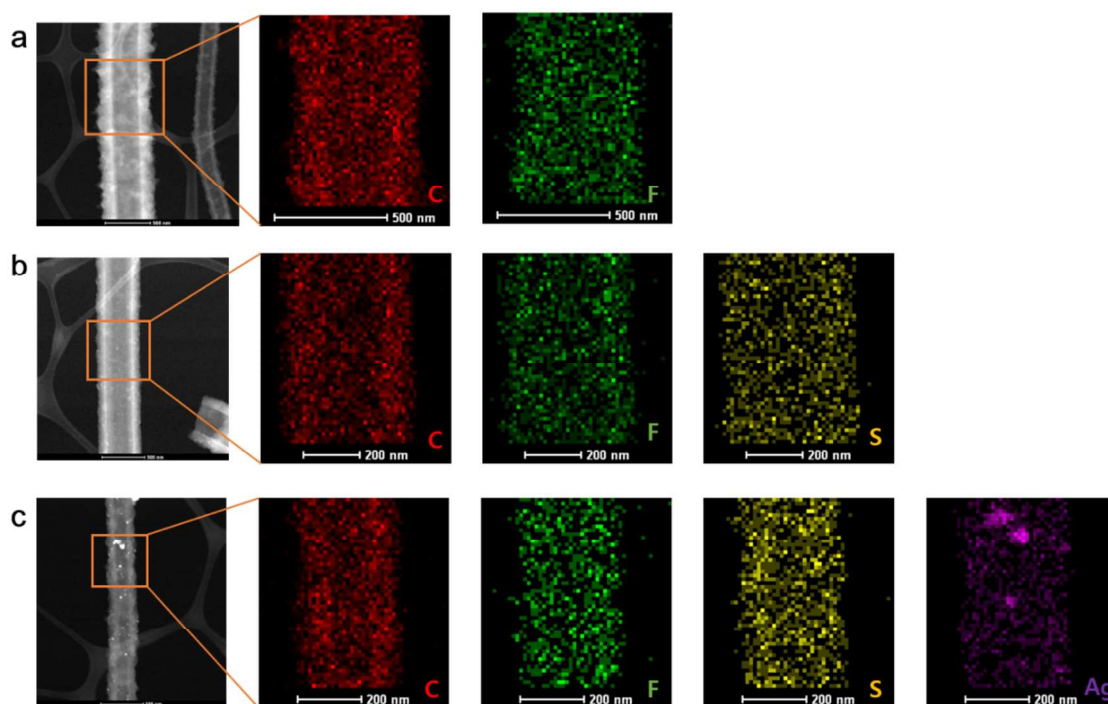


Figure S5. TEM-EDS elemental mapping of (a) the MOP sponge, (b) S-MOPS, and (c) S-MOPS-Ag.

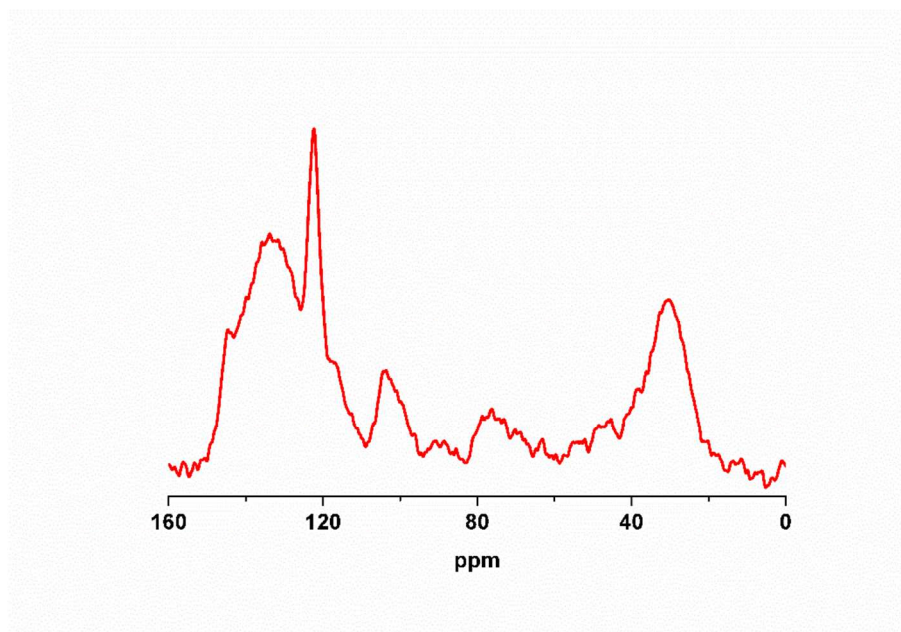


Figure S6. Solid state ^{13}C CP/MAS NMR spectrum of S-MOPS-Ag.

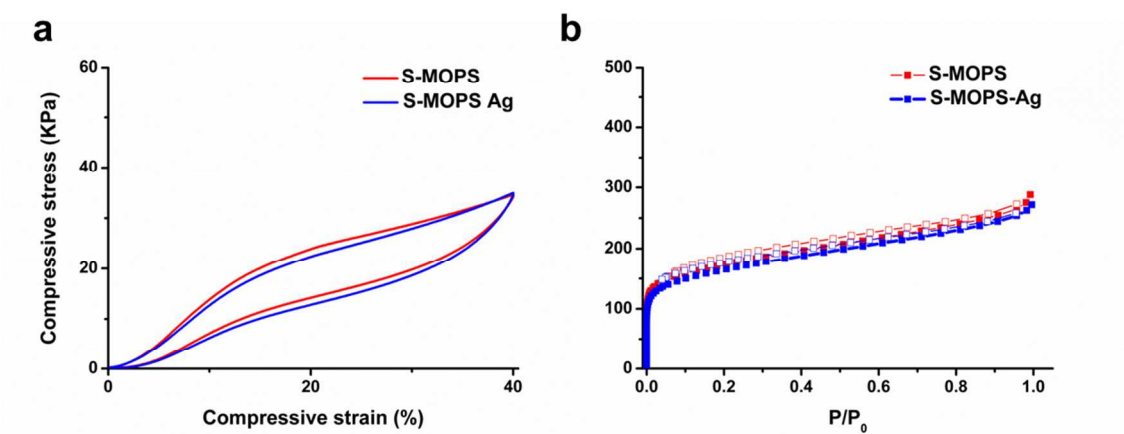


Figure S7. a) Compressive stress-strain curves (maximum strain = 40%) and b) N_2 adsorption-desorption isotherms measured at 77 K of S-MOPS and S-MOPS-Ag.

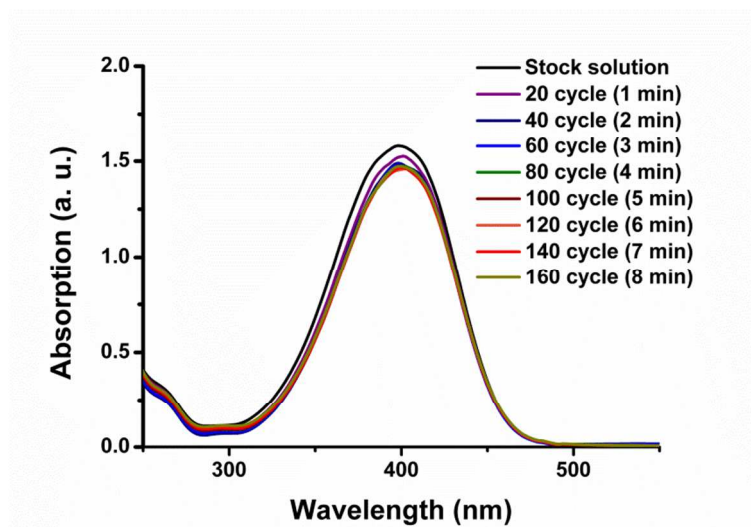


Figure S8. UV-Vis spectra of the aqueous 4-NP solution (initial concentration = 1×10^{-4} M) measured during the reaction with the repeated compression and release of S-MOPS.

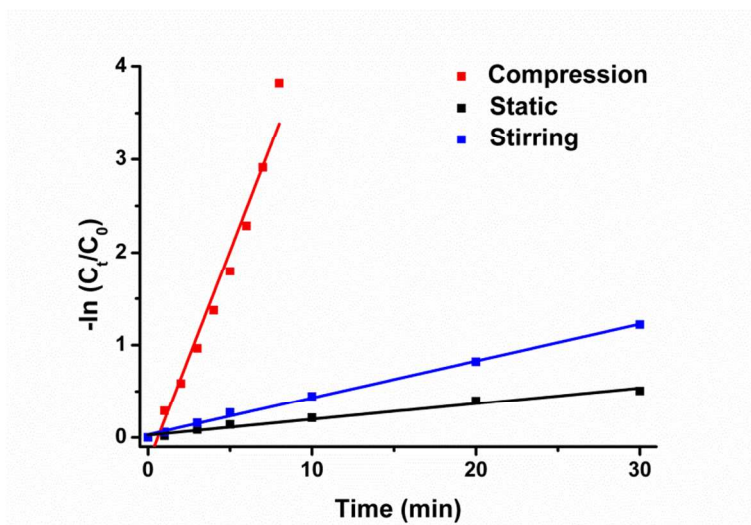


Figure S9. Plots of $-\ln(C_t / C_0)$ versus time during the catalytic reduction of 4-NP by S-MOPS-Ag under different reaction conditions. With the compression-release process, the apparent rates constant (k) for the reaction = $7.61 \times 10^{-3} \text{ s}^{-1}$. Without the compression and release process, $k = 2.84 \times 10^{-4} \text{ s}^{-1}$ when the reaction solution was not stirred and $k = 6.64 \times 10^{-4} \text{ s}^{-1}$ when the reaction solution was stirred.

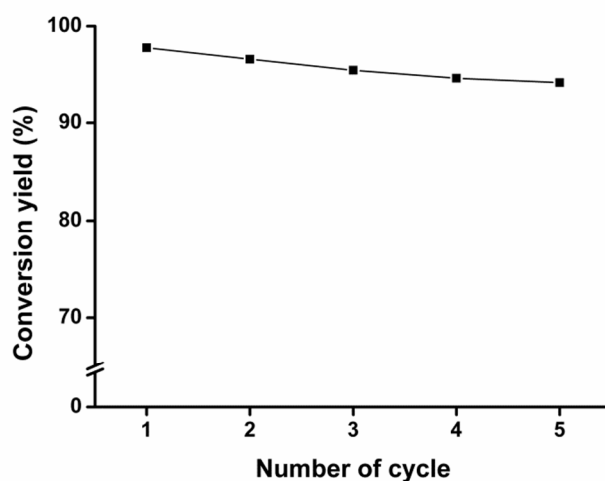


Figure S10. Change in the catalytic activity of S-MOPS-Ag during recycling.

References

- (1) Ye, Y.; Jin, M.; Wan, D. One-Pot Synthesis of Porous Monolith-Supported Gold Nanoparticles as an Effective Recyclable Catalyst, *J. Mater. Chem. A*, **2015**, 3, 13519–13525.
- (2) Katiyar, S.; Mondal, K.; Sharma, A. One-Step Sol–Gel Synthesis of Hierarchically Porous, Flow-Through Carbon/Silica Monoliths, *RSC Adv.*, **2016**, 6, 12298-12310.
- (3) Liu, H.; Wan, D.; Du, J.; Jin, M. Dendritic Amphiphile Mediated One-Pot Preparation of 3D Pt Nanoparticles-Decorated PolyHIPE as a Durable and Well-Recyclable Catalyst, *ACS Appl. Mater. Interfaces*, **2015**, 7, 20885–20892.